

Observation of coupled plasmon-polariton modes of plasmon waveguides for electromagnetic energy transport below the diffraction limit

Stefan A. Maier*, Pieter G. Kik, Mark L. Brongersma and Harry A. Atwater

Thomas J. Watson Laboratory of Applied Physics, California Institute of Technology,
Pasadena, CA 91125, USA

Sheffer Meltzer, Ari A.G. Requicha, and Bruce E. Koel

Laboratory for Molecular Robotics

University of Southern California,

Los Angeles, CA 90089, USA

*e-mail: stmaier@caltech.edu

Abstract

We study the influence of optical near-field interactions on the dipole surface plasmon resonance of Au nanoparticles in closely spaced particle arrays using finite-difference time-domain simulations. In particular, the resonance energies of the collective plasmon-polariton modes are determined for longitudinal and transverse polarization for different particle array lengths and inter-particle spacings of 50 nm Au spheres in air. The obtained results are set in context with recent publications suggesting the possibility to use ordered arrays of closely spaced noble metal nanoparticles as plasmon waveguides for electromagnetic energy below the diffraction limit of light.

Introduction

The optical properties of metal nanoparticles have been the focus of intense research for a number of years [1]. From work on single noble metal nanoparticles, it is well established that light at the dipole surface plasmon frequency interacts strongly with metal nanoparticles and excites a collective electron motion, or surface plasmon-polariton [2]. These plasmon resonances are typically in the visible or infrared part of the spectrum and exhibit plasmon decay times of a few femtoseconds [1]. For particles with a diameter D much smaller than the wavelength λ of the exciting light, plasmon excitations produce oscillating dipole fields.

Whereas until recently most work has focused on the optical properties of disordered arrays of large numbers of particles, advances in particle synthesis and fabrication now allow for an investigation of the optical properties of ordered arrays of metal nanoparticles and the effects of particle interactions on the plasmon resonance. Since each excited nanoparticle with a diameter $D \ll \lambda$ acts as an oscillating dipole, two types of inter-particle interactions can be distinguished: near-field coupling and far-field dipolar interactions. For particle spacings d larger than the wavelength λ of the exciting light, far-field dipolar interactions with a distance dependence d^{-1} dominate. Indeed, it has been shown that both the position and the linewidth of the plasmon resonance of ordered gratings of Au nanoparticles with grating constants of several 100 nm are influenced by far-field dipolar interactions [3]. Most work on ordered arrays has focused on these far-field particle interactions, and it has been shown that far-field interactions can lead to a surface plasmon polariton band gap on patterned Au surfaces [4]. But relatively little is known about the properties of near-field interactions between closely spaced metal particles with an

interparticle spacing d of a fraction of the wavelength λ . Recently it was suggested that chains of closely spaced noble metal nanoparticles could be used as waveguides for electromagnetic (EM) energy below the diffraction limit of light [5]. Guiding in these plasmon waveguides relies on near-field coupling between adjacent nanoparticles which sets up coupled plasmon modes. Analysis of Au nanoparticle chains using near-field optical microscopy has indeed shown signs of collective behavior of such chains [6]. Note that a spatial confinement of the guided waves below the diffraction limit cannot be achieved with band gap structures due to the inherent periodicity on the order of the wavelength λ .

In a number of recent publications, we have experimentally demonstrated guiding of EM energy below the diffraction limit in macroscopic analogs to plasmon waveguides operating in the microwave regime [7, 8]. We further presented a point-dipole model for the guiding properties of nanoscale plasmon waveguides [9, 10], which allowed for a determination of the dispersion relation and the group velocity for energy transport. Far-field spectroscopy on fabricated structures consisting of closely spaced Au nanoparticles confirmed the predictions of the dipole model for the long-wavelength in-phase mode of a plasmon waveguide [11].

In order to optimize the guiding parameters of plasmon waveguides using different particle geometries and spacings, a detailed knowledge of the properties of the near-field interactions between closely spaced metal nanoparticles is desirable. In this paper, we present an analysis of the near-field interactions of ordered arrays of Au nanoparticles with an interparticle spacing d much smaller than the wavelength of light using finite-difference time-domain (FDTD) simulations. In particular, we discuss the dependence of the plasmon resonance frequency for the long-wavelength mode of plasmon waveguides for different nanoparticle chain lengths and interparticle spacings and present an assessment of the expected group velocity and waveguide loss.

Simulations

We investigate the optical response of ordered arrays of closely spaced 50 nm Au spheres in air using FDTD simulations. In order to accurately model the material properties of Au, the dispersive behavior at visible frequencies has to be taken into account. Fig. 1 shows the literature values for the frequency-dependence of the real part ϵ_1 of the dielectric function for Au obtained by measurements on bulk Au samples (squares) [12] and 30 nm Au spheres (circles) [13].

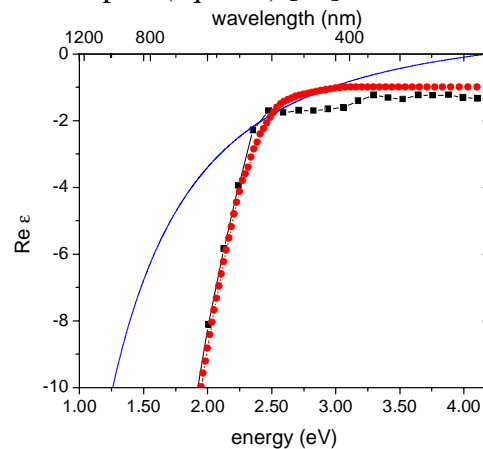


Figure 1. Real part ϵ_1 of the dielectric function of Au obtained from measurements on bulk Au samples (black squares) and 30 nm Au nanospheres (red circles). Also shown is the functional form of the Drude model (blue line) used to approximate ϵ_1 around $\epsilon_1 = -2$.

The close agreement between both datasets implies that the real part of the dielectric function of Au nanoparticles with diameters $D > 30\text{nm}$ can be modeled using bulk values. However, the imaginary part ε_2 of the dielectric function of Au nanoparticles with diameters $D < 50\text{ nm}$ does differ appreciably from the bulk values due to increased damping caused by surface scattering of the oscillating electrons [13]. This has to be taken into account via an increased electron scattering time τ .

Our FDTD simulation approach allows us to model the dielectric response of Au nanoparticles using a Drude model with a dielectric constant

$$\varepsilon_1(\omega) = 1 - \frac{\omega_p^2}{\omega^2 + \Gamma^2}. \quad (1)$$

The free parameters to model the dielectric response of Au are the bulk plasmon frequency ω_p and the free electron scattering frequency Γ . We chose $\omega_p = 6.79 \times 10^{15}\text{ rad/s}$ in order to obtain a close match between the Drude model and the measured data around $\varepsilon_1 = -2$, which is the plasmon resonance condition of small spheres in air. In order to model typical plasmon decay times τ of 4 fs for Au nanoparticles [2], we set the scattering frequency $\Gamma = 2.5 \times 10^{14}\text{ rad/s}$.

Fig. 2 describes our simulation approach for the determination of the dipole surface plasmon frequencies of Au nanoparticles for the case of a single Au sphere with a diameter of 50 nm in air. The simulation volume consists of a rectangular box of dimensions 1000 nm x 400 nm x 400 nm with the 50 nm Au sphere placed at the center as shown in the inset of Fig. 2a. This box is overlaid with a rectangular grid of 1 million mesh points using a graded mesh density to ensure a high density of points near the particle. The dipole surface plasmon resonance of the nanoparticle is then determined using two simulation runs. In a first run, the nanoparticle is illuminated with a plane-wave propagating in the z-direction with the electric field polarized in the x-direction as

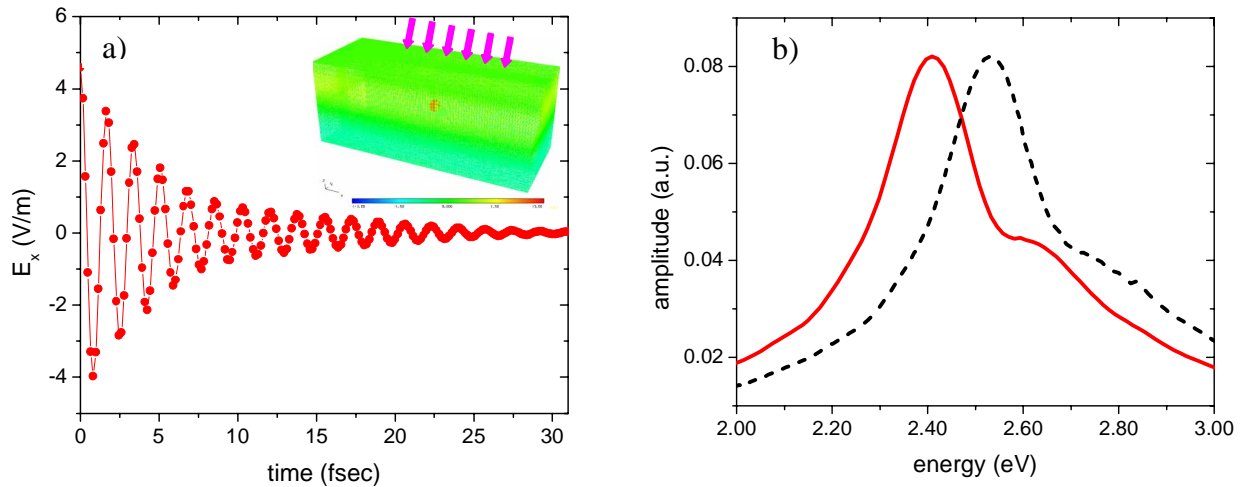


Figure 2. a) The inset shows the x-component the electric field for a normal incidence plane-wave illumination of the simulation volume with a 50 nm Au sphere at the center. The plane wave sets up an enhanced electric field inside the particle (red color). The main graph shows the oscillatory decay of the enhanced field $\mathbf{E}(t)$ at the center of the nanoparticle after the plane-wave is switched off. b) Fourier – Transform of $\mathbf{E}(t)$ with the dipole surface plasmon peak at 2.4 eV (red line). Also shown is the corresponding peak for a 10 nm Au sphere at 2.53 eV (black dotted line).

shown in the inset of Fig. 2a. The frequency of the plane wave was chosen to be 6×10^{14} Hz (2.48 eV), as will be discussed below. The plane-wave illumination leads to the build-up of an oscillating homogeneous electric field inside the nanoparticle. A snapshot of the electric field distribution inside the simulation volume is used as the initial field condition for a second simulation run without any external sources. Fig. 2a shows the time evolution of the field at the center of the nanoparticle. The field decays in a damped harmonic oscillation $\mathbf{E}(t)$ with the damping constant corresponding to the relaxation time τ of the Drude model. The Fourier transform of $\mathbf{E}(t)$ shown in Fig. 2b (red line) displays a single dipole peak centered at 2.4 eV. This peak corresponds to the position of the surface plasmon dipole resonance of the 50 nm Au sphere in air. The resonance is red-shifted compared to the dipole resonance of a “small” Au particle at 2.58 eV obtained from quasistatic Mie-theory [1]. This red-shift is caused by radiation damping of the plasmon resonance since the particle diameter D of 50 nm is an appreciable fraction of the wavelength, so that the condition $D \times \lambda \ll 1$ for the quasistatic approximation does not hold anymore. To verify our calculation method, we also calculated the resonance for a 10 nm Au sphere (black dotted line). In this case the dipole resonance is centered at 2.53 eV, close to the quasistatic value of 2.58 eV, demonstrating the validity of our model.

Two points regarding our simulation approach should be noted. First, the frequency of the plane wave chosen for the build-up of the initial electric field in the first simulation run does not need to be close to the plasmon resonance frequency of the investigated nanostructure in order to obtain the right position of the resonance peak, as was confirmed by a simulation run with a frequency of 3×10^{14} Hz (1.24 eV). However, a frequency close to the resonance leads to the build-up of a higher field inside the nanostructure than outside, which reduces surface polarization effects due to the initial outside field. This was seen to improve the shape of the dipole peak obtained by Fourier transform while not altering its peak position. Second, our model does not take into account a decrease in the width of the dipole resonance due to peak shifts to lower frequencies away from the onset of the interband transitions of bulk Au. This is due to the fixed electron relaxation time τ of the Drude model.

Figure 3 shows the position of the plasmon resonances of 50 nm Au spheres in air in nanoparticle chains of different lengths and inter-particle spacings for polarizations along (longitudinal modes L, black squares) and perpendicular (transverse modes T, red circles) to the chain axis. Since all the particles constituting the chains are excited in phase, the plasmon resonances correspond to collective longitudinal and transverse modes of the chain as a whole. Fig. 3a shows the resonance positions for both polarizations for particle chains with up to 6 particles with an inter-particle center-to-center spacing of 75 nm, corresponding to $1.5D$. These resonance positions are the average of the resonance frequencies obtained for each nanoparticle in the chain. In the case of a single Au sphere, the longitudinal and transverse resonances coincide at position E_0 due to its spherical symmetry. For increasing particle chain lengths, the plasmon resonance peak E_L (for L polarization) shifts to lower and the peak E_T (for T polarization) to higher frequencies due to near-field interactions between the particles. The peak splitting $\Delta E = |E_T - E_L|$ saturates for particle chain lengths of 5 particles at $\Delta E \approx 200$ meV. The fact that the splitting has not yet saturated for particle chains of 3 particles shows that the coupling is not governed by nearest-neighbor interactions alone. Our results qualitatively agree with calculations for the interaction of silver nanoparticles based on Mie-theory [14].

Figure 3b shows the dependence of the plasmon peaks $E_{L,T}$ for chains of 5 Au spheres with a diameter of 50 nm on interparticle spacing d . The bandwidth is seen to decrease with increasing interparticle spacing as d^{-3} , and for $d = 175$ nm ($3.5 D$) the peaks practically coincide ($\Delta E \approx 0$).

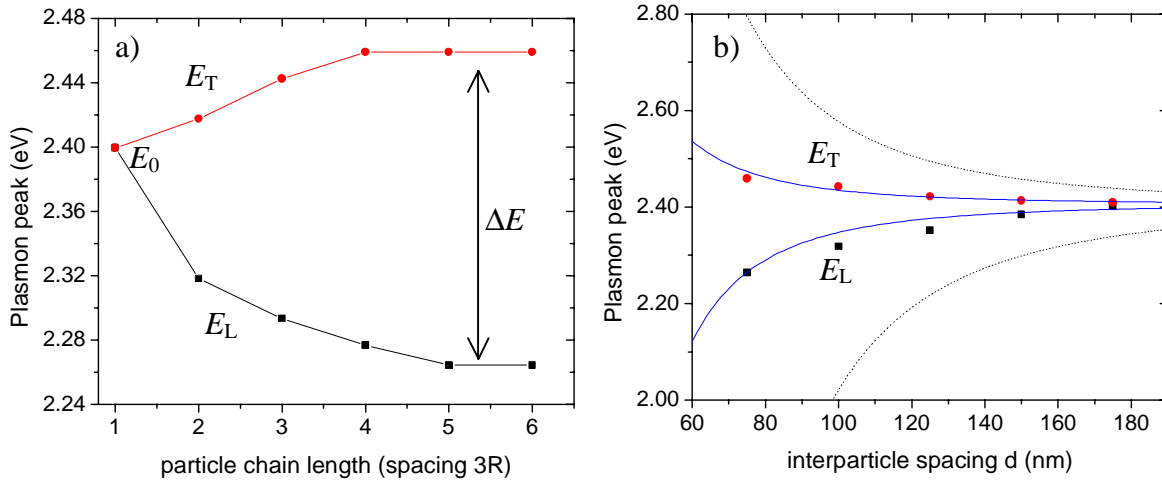


Figure 3. Position of the dipole resonance of 50 nm Au spheres in nanoparticle chains for a polarization along (longitudinal mode L, black squares) and perpendicular (transverse mode T, red circles) to the chain axis. a) Dependence on particle chain length with an inter-particle spacing of 75 nm. b) Dependence on inter-particle spacing for a chain length of 5 particles. Also shown is the dependence calculated using the dipole-model of Ref. 8 for surrounding media with $n=1$ (black dotted line) and $n=2.5$ (blue solid line)

This strong dependence of the peak splitting ΔE on the interparticle spacing is characteristic for near-field interactions. Also shown are the functional dependencies for $E_{L,T}$ on the inter-particle spacing as predicted by the dipole model for plasmon waveguides [9] of our geometry (black dotted line). While the decrease of the peak splitting with increasing interparticle spacing can be well described with the point-dipole model, the absolute magnitude of the splitting is clearly overestimated. A point-dipole model with a coupling strength reduced by a factor 6.25 (corresponding to particles embedded in an effective medium with $n = 2.5$) fits the experimental data well (blue solid line). We attribute this reduced coupling strength to the fact that the 50 nm Au spheres do not behave as perfect point dipoles due to their extended charge distributions. In order to experimentally verify the predictions of the FDTD simulations for the peak splitting ΔE between the modes, we fabricated plasmon waveguides corresponding to the simulated geometries using electron beam lithography. Far-field extinction measurements of the collective modes showed a good match with the simulations as described here [11, 15].

The extracted values for the peak splitting ΔE between the L and T modes of nanoparticle chains are a direct measurement of the inter-particle coupling strength and thus allow for the calculation of the expected group velocity and energy propagation loss in plasmon waveguides [11, 15] using the functional form of the dispersion relation for energy transport of the point-dipole model [9]. Our FDTD simulations predict a maximum group velocity of 1.6×10^7 m/s for the longitudinal mode and a plasmon amplitude damping constant $\alpha = 7.81 \times 10^6 \text{ m}^{-1}$, corresponding to an energy decay length of about 3 dB / 50 nm. The magnitude of the calculated group velocity and energy decay length are about one order of magnitude lower than the predictions of the point-dipole model [9], due to the decreased near-field coupling strength as discussed above.

A use of plasmon waveguides as means for energy transport in nanoscale optical circuits would require a reduction of the damping constant by one order of magnitude in order to allow

for guiding of EM energy over distances of several hundred nanometers. This can be achieved either via an increase in near-field coupling strength or a decrease in the particle plasmon damping time τ . Both goals can be achieved for Au particles by a geometry change that red-shifts the plasmon resonance away from the interband transition edge, as is discussed elsewhere [15, 16].

Conclusions

Finite-difference time-domain simulations were used to study optical near-field interactions between closely spaced Au nanoparticles. An investigation of the peak splitting ΔE between the longitudinal and transverse mode of collective excitation for chains of Au spheres with a diameter of 50 nm and an inter-particle spacing of 75 nm showed the peak splitting to saturate at $\Delta E \approx 200$ meV for chain lengths of 5 particles. This peak splitting corresponds to a maximum group velocity of about 0.05 c and an energy damping of about 3 dB/50nm for energy transport.

Acknowledgement

This work was supported by the National Science Foundation via award ECS0103543 and the Center for Science and Engineering of Materials at Caltech.

References

1. U. Kreibig and M. Vollmer, *Optical Properties of Metal Clusters* (Springer-Verlag, Berlin, 1994)
2. T. Klar, M. Perner, S. Grosse, G. von Plessen, W. Sprickl, and J. Feldmann, *Phys. Rev. Lett.* **80**, 4249 (1998)
3. B. Lamprecht, G. Schider, R.T. Lechner, H. Ditlbacher, J.R. Krenn, A. Leitner, and F.R. Aussenegg, *Phys. Rev. Lett.* **84**, 4721 (2000)
4. Sergey I. Bozhevolnyi, John Erland, Kristjan Leosson, Peter M.W. Skovgaard, and Jorn M. Hvam, *Phys. Rev. Lett.* **86**, 3008 (2001)
5. M. Quinten, A. Leitner, J.R. Krenn, and F.R. Aussenegg, *Optics Letters* **23**, 1331 (1998)
6. J.R. Krenn, A. Dereux, J.C. Weeber, E. Bourillot, Y. Lacroute, J.P. Goudonnet, G. Schider, W. Gotschy, A. Leitner, F.R. Aussenegg, and C. Girard, *Phys. Rev. Lett.* **82**, 2590 (1999)
7. S. A. Maier, M.L Brongersma, and H.A. Atwater, *Appl. Phys. Lett.* **78**, 16 (2001)
8. S.A. Maier, M.L. Brongersma, and H.A. Atwater, *Material Science and Engineering C* **19**, 291 (2002)
9. M.L. Brongersma, J.W. Hartman, and H.A. Atwater, *Phys. Rev. B* **62**, R16356 (2000)
10. S.A. Maier, M.L. Brongersma, P.G. Kik, S. Meltzer, A.A.G. Requicha, and B.E. Koel, *Adv. Mat.* **13**, 1501 (2001)
11. S.A. Maier, M.L. Brongersma, P.G. Kik, and H.A. Atwater, *Phys. Rev. B* **65** (to be published 2002)
12. P.B. Johnson and R.W. Christy, *Phys. Rev. B* **6**, 4370 (1972)
13. M. Quinten, *Zeitschrift für Physik B* **101**, 211 (1996) and private communication
14. M. Quinten, *Applied Optics* **32**, 6173 (1993)
15. S.A. Maier, P.G. Kik, and H.A. Atwater, *Appl. Phys. Lett.* (submitted)
16. C. Sönnichsen, T. Franzl, T. Wilk, G. von Plessen, and J. Feldmann, *Phys. Rev. Lett.* **88**, 077402 (2002)